Uncertainty Analysis of GIRM by Stochastic Sampling Method

Somyung Park[a], Hyun Chul Lee [a*]
[a]*School of Mechanical Engineering, Pusan National University, 2, Busandaehak-ro 63beon-gil, Geumjung-gu, Busan, 46241, Republic of Korea*
[*]*Corresponding author: hyunchul.lee@pusan.ac.kr*

Keywords : Graphite Isotope Ratio Method (GIRM), Uncertainty quantification, Nuclear cross section covariance data, Stochastic sampling, McCARD

1. Introduction

The Graphite Isotope Ratio Method (GIRM) was developed by the Pacific Northwest National Laboratory (PNNL) in the 1990s. The GIRM provides a means to predict plutonium production in graphite-moderated reactors. During reactor operation, impurities in graphite are transmuted, and simultaneously, plutonium is produced in fuel. Consequently, a correlation exists between these two processes which the GIRM utilizes. This method remains effective even in the absence of detailed operational histories. [1-5]

Various studies have been conducted to validate the GIRM. However, studies on the uncertainty associated with GIRM remain limited. There are two primary methods for uncertainty quantification analysis. One is a deterministic method, such as Sensitivity/Uncertainty (S/U) analysis [6,7], and a stochastic method involving randomly sampling of input parameters. [8,9] In a previous study, the GIRM validation experiment conducted at HANARO research reactor was simulated using a Monte Carlo code McCARD developed by Seoul National University (SNU). [10] This experiment utilized graphite and nuclear fuel specimens. The impurities in the graphite specimens varied; among them, Boron, Iron, Titanium, Tungsten, and Uranium were used as indicator isotopes. The experimental setup included three jigs, each consisting of two sets of graphite specimens and one set of nuclear fuel specimens. The specimens were loaded into the experimental instrument consisting of jig and then subjected to irradiation testing. The jigs and rods are categorized according to their positions. The index of the Jig indicates axial position of the jig, with they loaded in the order of their indices, while the index of the rod represents its position in the radial direction as shown in Fig. 1. The indicator isotope ratios in the graphite specimens of each set and the plutonium production in nuclear fuel specimens in each jig were evaluated through burnup calculations. The uncertainty factors for the GIRM were estimated based on manufacturing tolerance of experiment instruments and stochastic errors from MC calculation using different random seed numbers. [11] Additionally, uncertainties in nuclear cross sections, which are correlated with other reactions, were considered leading to uncertainties in cross section.

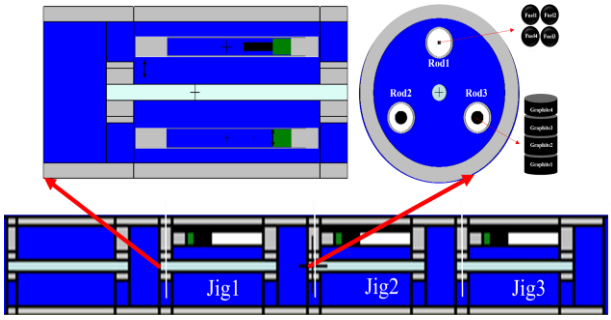

Fig. 1. The diagram of experimental instrument consisting of Jig with marked indexing

In this paper, total uncertainties due to uncertainties in cross section and stochastic errors were quantified using a random sampling module developed by Professor Park.[12]. These errors were estimated through regression analysis of the correlation between the isotope nuclides ratios and cumulative plutonium amounts.

2. Methods

One hundred independent McCARD simulations, each with different a random seed number, were conducted to account for cross section covariance data. Polynomial regression was used to generate regression curves, and the residuals between MC calculation results and regression data were analyzed for uncertainty quantification. This section details the stochastic sampling method that incorporates cross section covariance data into the final calculations and statistical analysis.

2.1 Stochastic sampling method

Cross sections are correlated with each other, which can be represented using a covariance matrix. The random sampling is performed by decomposing the covariance matrix. [12] Let A be the covariance matrix, and L be the matrix obtained through spectral decomposition. According to spectral decomposition, the matrix Λ is a diagonal matrix consisting of eigenvalues, and the matrix P contains the eigenvectors arranged in columns corresponding to the eigenvalue order of Λ. Since the covariance matrix is symmetric and positive definite, P^T is the transpose of P. Therefore, the decomposed matrix L is defined as $L = P\sqrt{\Lambda}$, and

covariance matrix A can be decomposed as shown in Equation (3).

$$A = P\Lambda P^T \cong LL^T \quad (1)$$

Random sampling is preformed using Equation (2). In this context, $\bar{X}$ represents the averaged cross section vector, and Z denotes a random normal vector obtained by sampling from the standard normal distribution using the Box-Muller method. [12]

$$X' = \bar{X} + L \cdot Z \quad (2)$$

2.2 Cross section sampling configuration

In this paper, the raw covariance matrix of the nuclear cross sections was calculated using the ERROR module of the NJOY program [13] with ENDF/B-VII.1 files. The energy group for generating the covariance matrix was set to the SCALE6 44-energy-group format. Various nuclides and nuclear reactions were selected to assess the impact of cross section uncertainty on the GIRM. The nuclides related to plutonium production and those associated with nuclear reactions of indicator were selected. The covariance matrices for 14 nuclides were generated, focusing on key nuclear reactions for each nuclide. In particular, the covariance data for ^{10}B included (n, α) reactions. The summary for covariance data is provided in Table I.

Table I. Summary of reaction type of Covariance matrix by nuclides.

Nuclide	Reaction Type
^{10}B	Capture (MT102) (n, α) (MT107) Elastic Scattering (MT2) Inelastic Scattering (MT4)
^{11}B, ^{48}Ti, ^{49}Ti, ^{54}Fe, ^{56}Fe, ^{57}Fe, ^{182}W, ^{183}W,^{149}Sm,	Capture (MT102) Elastic Scattering (MT2) Inelastic Scattering (MT4)
^{235}U,^{238}U ^{239}Pu,^{240}Pu	Fission (MT18) Capture (MT102) Elastic Scattering (MT2) Inelastic Scattering (MT4) ν (MT452)

2.3 Statistical processing

The cumulative plutonium production and isotope ratios at each burnup step are calculated based on the MC code and each sampled input set. The polynomial regression with a logarithmic transformation of isotope ratio data is employed to identify the correlation between plutonium production and the isotope ratio. The regression curve is determined using the least squares method as shown in Equation (3).

$$y_{r,i}^k = \sum_j^3 a_i (\log x_i)^j \quad (3)$$

$y_{r,i}^k$ represents the regression cumulative plutonium mass density for the k-th sampled input set, and the i denotes the index of indicator nuclide. The regression order is set to 3, with x_i indicatng the isotope ratio of the *i-th* indicator nuclide. Accordingly, $y_{mc,i}^k$ represents the cumulative plutonium mass density obtained from k-th Monte Carlo (MC) calculation. The uncertainty of plutonium production associated with each indicator nuclide can be defined as shown in Equation (4).

$$\sigma_i^2 \cong \frac{1}{K-1} \sum_{k=1}^K (y_{mc,i}^k - y_{r,i}^k)^2 \quad (4)$$

3. Results

3.1 Verification for random sampling

The validity of sampling cross section considering the covariance matrix was confirmed by calculating the covariance of sample sets. Three sample set sizes were used: 100, 1000, and 10000 samples. To facilitate clearer comparison, the covariance matrix was converted into a correlation coefficient matrix for visualization. The correlation coefficient matrix was generated by dividing each element by the root mean square of the diagonal elements corresponding to the row and column indices. The overall correlation coefficient matrices consist of correlation coefficient matrices arranged diagonally in the order of fission, capture, elastic scattering, inelastic scattering reactions, and ν. In this paper, the verification results for two nuclides, ^{235}U and ^{238}U, are shown in Fig. 2 and Fig. 3. The correlation coefficient outside black box represents correlations between reactions that belong to the same row and column. As the number of sample sets increases, the correlation coefficient matrix from sample sets increasingly approximates the raw matrix. This demonstrates that the stochastic sampling method works effectively and has been consistently applied to other nuclides.

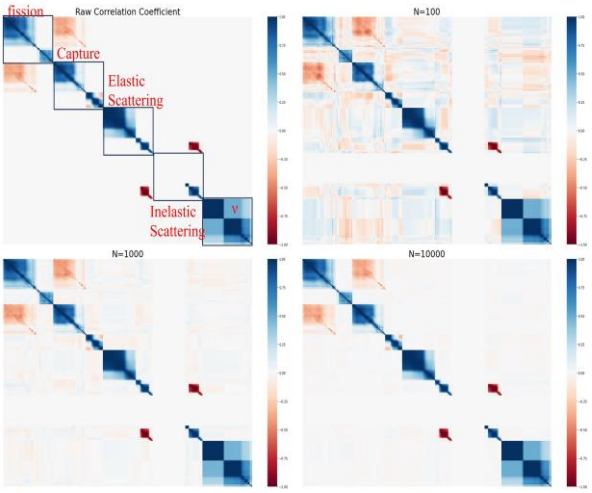

Fig. 2. Comparison between raw correlation coefficient and correlation coefficient matrices sampled for ^{235}U.

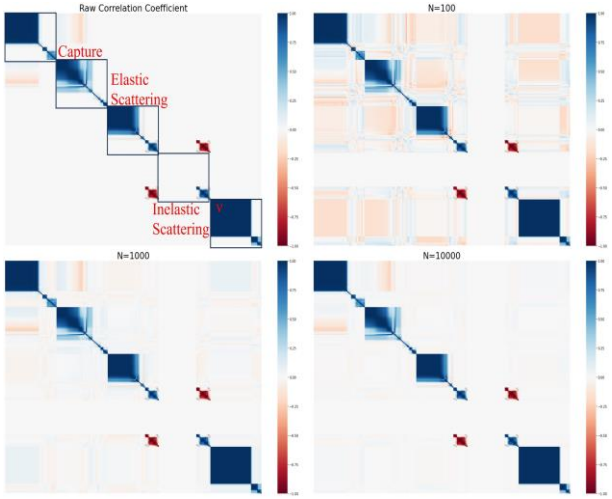

Fig. 3. Comparison between raw correlation coefficient and correlation coefficient matrices sampled for ^{238}U.

3.2 Polynomial Regression

In this paper, the regression curves and sampling data for boron case are visualized in Fig 4. The blue dots represent cumulative plutonium production for each isotope ratio data, while the red line denotes the regression line obtained using polynomial regression, as described in Section 2.3. The blue dots were sampled from 23 burnup points ranging from 28 to 336 Effective Full Power Days (EFPDs). Each subfigure illustrates regression results and Monte Carlo (MC) results categorized by sampling locations. The coefficients of determination (R^2) of boron, uranium, and Titanium cases exceed 0.990. However, in the iron and tungsten cases, the coefficients of determination are relatively lower, with most values falling below 0.990, and the distribution of the MC results is also more spread out, as shown in Fig. 5. Detailed coefficients of determination for all indicator nuclide cases are provided in Table 2.

Table II. Summary table for the coefficients of determination (R^2) for each indicator nuclide cases.

Indicator nuclides	index	R^2 with Rod2	index	R^2 with Rod3
Boron	Jig1	0.99577	Jig 1	0.99579
	Jig 2	0.99481	Jig 2	0.99480
	Jig 3	0.99409	Jig 3	0.99412
Titanium	Jig1	0.99381	Jig 1	0.99382
	Jig 2	0.99289	Jig 2	0.99290
	Jig 3	0.99118	Jig 3	0.99119
Iron	Jig1	0.98764	Jig1	0.98770
	Jig 2	0.98766	Jig 2	0.98775
	Jig 3	0.98512	Jig 3	0.98512
Tungsten	Jig1	0.99159	Jig1	0.99151
	Jig 2	0.98973	Jig 2	0.98974
	Jig 3	0.98980	Jig 3	0.98964
Uranium	Jig1	0.99569	Jig1	0.99571
	Jig 2	0.99470	Jig 2	0.99470
	Jig 3	0.99401	Jig 3	0.99405

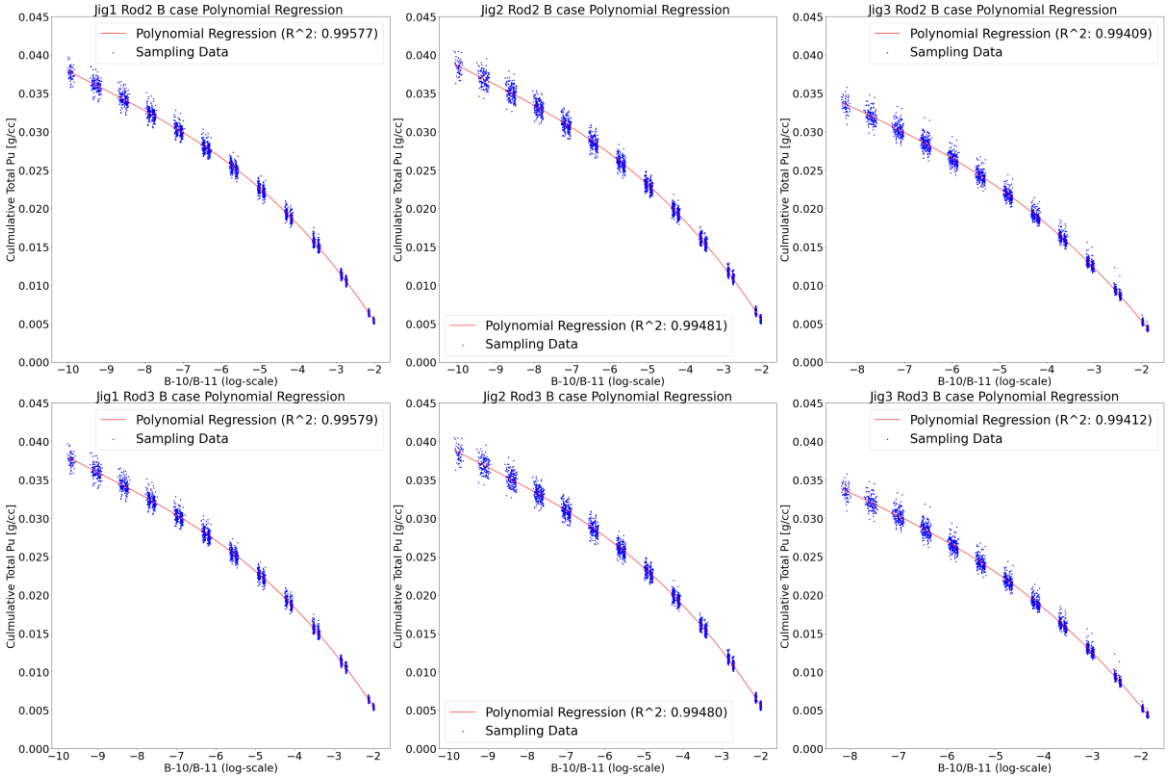

Fig. 4. Polynomial regression curves of 3 order and cumulative plutonium gram density for each independent MC calculations in the Boron cases.

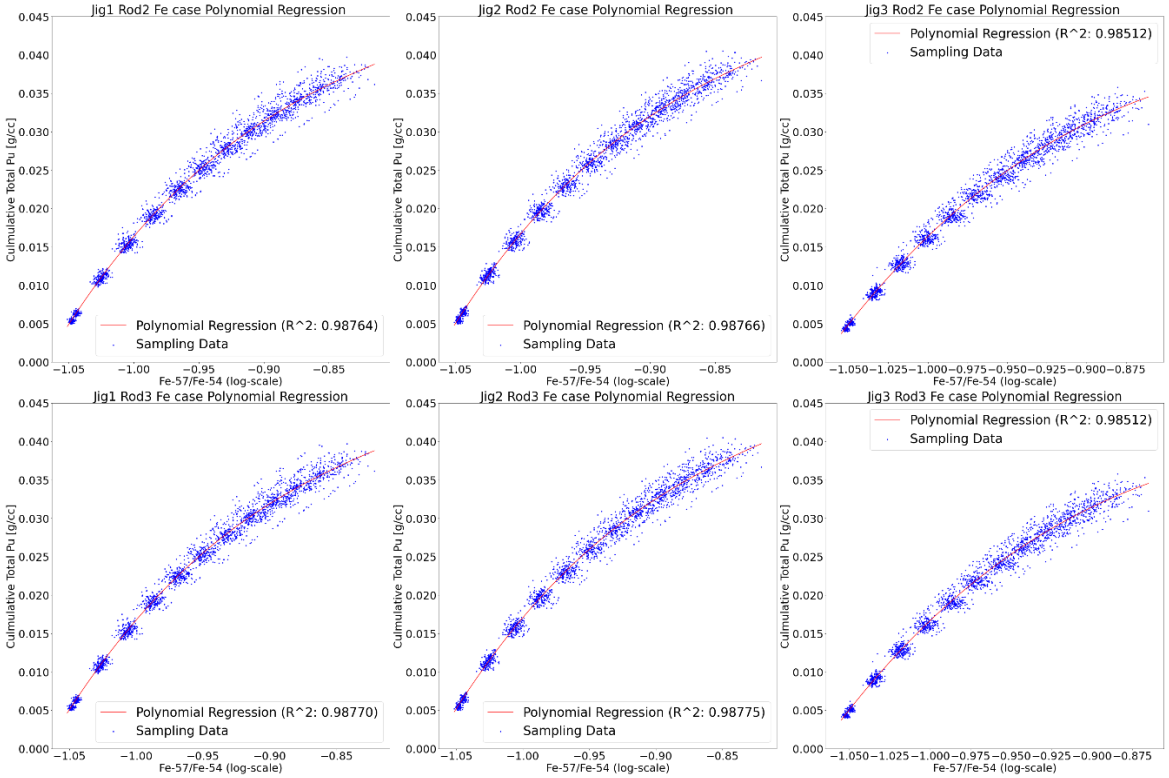

Fig. 5. Polynomial regression curves of 3 order and cumulative plutonium gram density for each independent MC calculations in the Iron cases.

3.3 Uncertainty analysis

The uncertainty, as calculated and described in Section 2.3, was normalized by dividing by the average of MC results for each burnup step to allow for a clearer estimation. Fig. 6. illustrates the total uncertainty based on stochastic errors and nuclear cross section covariance data. The uncertainty curves for each indicator nuclide are plotted over a range from 28 to 336 days. The subfigure illustrates the result categorized by sampling locations.

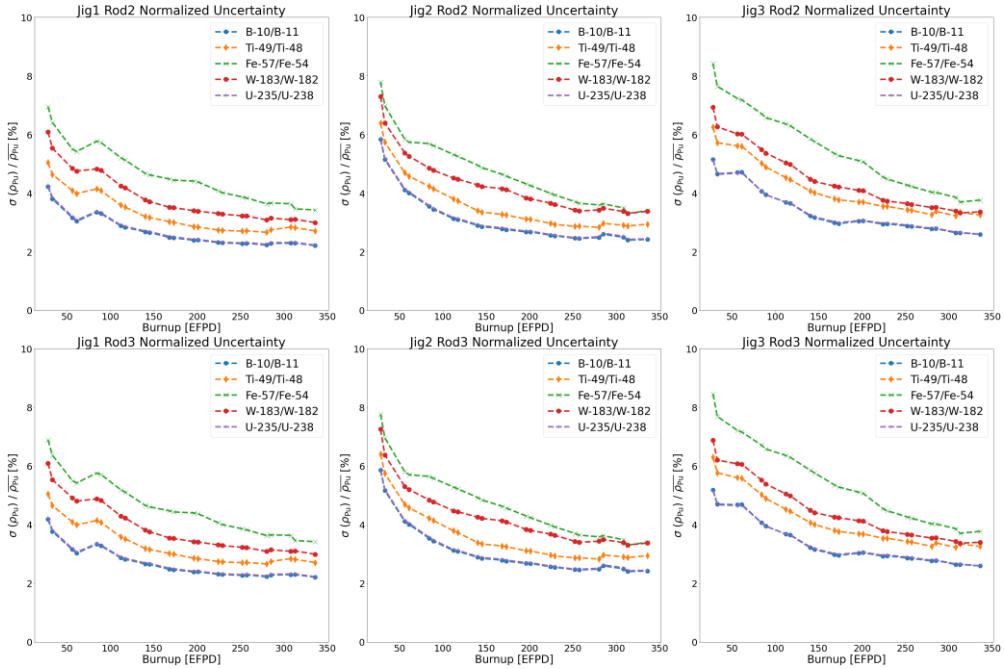

Fig. 6. Summary of normalized uncertainties according to every indicator nuclide considering cross section covariance data.

The results considering only stochastic error of the MC code initially range from 5% to 6%, eventually dropping by around 1% to 2%. [11] The total uncertainties considering cross section covariance data differed from results considering only stochastic error, and the results varied depending on the indicator nuclides. This indicates that the covariance data of the nuclear cross section influences the Total uncertainty as shown in Equation (5)

$$\sigma_{tot}^2 = \sigma_{Sto}^2 + \sigma_{XS}^2 \quad (5)$$

To estimate the uncertainty due to nuclear cross section covariance data, the uncertainties associated with stochastic errors were subtracted from the total uncertainties, as shown in Equation (6). Fig. 7 shows the results of this simple cross section uncertainty estimation for each indicator nuclide at every sampling location.

$$\sigma_{XS}^2 = \sigma_{tot}^2 - \sigma_{Sto}^2 \quad (6)$$

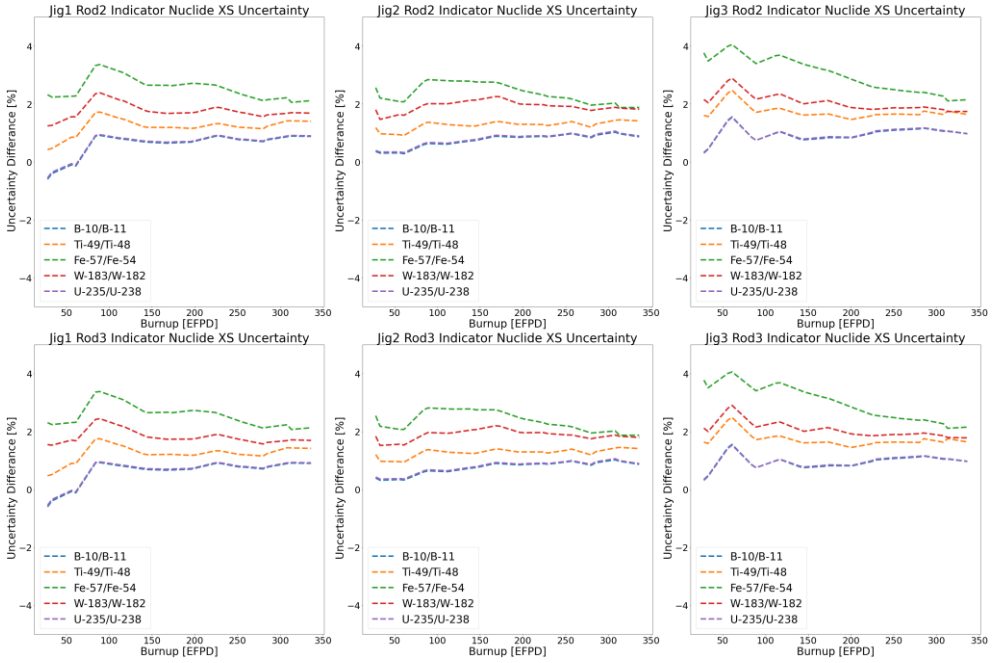

Fig. 7. Estimated uncertainties of cross section obtainted by simply subtracting the uncertainties by stochastic error to the total uncertainties

The results of the simple subtraction for the boron and uranium cases in the Rod2 and Rod3 of Jig1 initially show negative values. In constrast, the remaining cases exhibit positive results. To analyze these results, the relative standard deviations of cross sections were calculated by dividing the group standard deviations by the group cross secions obtained from NJOY. Fig. 8 presents relative standard deviations of key nuclear reaction cross sections for indicator nuclides in the thermal region. The relative standard deviations for the boron and uranium cases are below 1 %. Therefore, impact of stochastic errors appears to be more significant, resulting in some negative results when comparaing the total uncertainty with the uncertainty due to stochastic errors at the initial burnup step. At the initial burnup, the uncertainty due to stochastic errors is also estimated to be large due to small amount of plutonium. In the other cases, the total uncertainties were estimated in the order shown in Fig. 8. Since the effect of stochastic errors remains dominant, the results do not match those shown in Fig. 8.

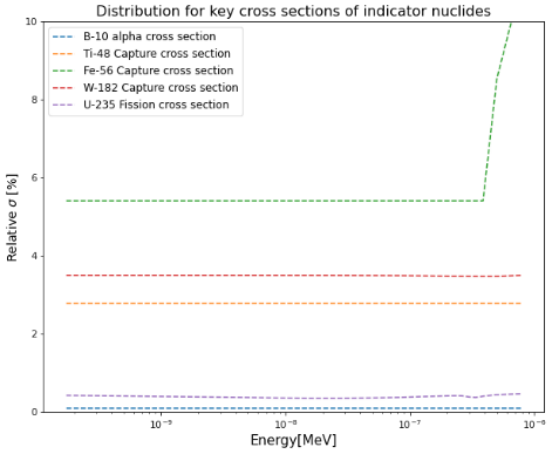

Fig. 8. The relative standard deviation of key cross sections of indicator nuclides affecting GIRM.

4.Conclusion

In this study, the stochastic sampling to account for uncertainty of nuclear cross sections was implemented using spectral decomposition and the Box-Muller sampling method. The coefficients of determination and uncertainties of all indicator nuclide cases were estimated to be at similar levels within the same Jig, regardless of the position of the graphite specimens. The total uncertainties for the Fe case start at approximately 8% at 28 days and decrease to about 4% at 336 days, while the Ti and W cases show a change from around 7% to 3%. For the other cases, uncertainties start at around 6% and decrease to about 2% by the final point. The uncertainties when considering only stochastic errors in the Monte Carlo (MC) calculation differed significantly. This suggests that the observed changes in total uncertainty can be attributed to the uncertainty in nuclear cross sections and secondary effects by using the several nuclear cross section covariance data. The total uncertainties vary depending on indicator nuclide cases. This is because the uncertainties associated with key cross sections vary for each indicator nuclide. The uncertainties of Fe case were estimated to be the largest because of large relative standard deviation of Fe key cross sections, followed by W and then Ti.

However, there was still a significant stochastic error from MC results, which made it challenging to analyze the detailed impact of due to covariance data. Especially, the uncertainties of boron and uranium cases exhibit very small standard deviation of cross sections, and it is difficult to analyze uncertatainties due to large stochastic errors. Therefore, it is necessary to reduce the stochastic error by MC calculations to analyze the effects of the covariance data in more detail. In the future work, a small-scale model focusing solely on the experimental area is planned. A detailed uncertainty analysis using covariance data for each nuclide will be conducted with this small-scale model.

Acknowledgments

The authors thank Ho Jin Park for providing random sampling module of McCARD used in this strudy. This research was supported by the National Research Foundation of Korea (NRF) grant funded by the Korea government (MSIT). (No.NRF-2019R1A2C2089962)

REFERENCES

[1] J. Kang, “Using the Graphite Isotope Ratio Method to Verify the DPRK’s plutonium-production Declaration”, Science and Global Security, Vol.19, p. 121-129, (2011).
[2] J.P. McNeece, et al., “The Graphite Isotope Ratio Method (GIRM): A Plutonium Production Verification Tool”, PNNL-12095, Pacific Northwest National Lab, (1999).
[3] B.D. Reid, W.C. Morgan, E.F. Love, Jr, D.C. Gerlach, S.L. Petersen, J.V. Livingston, L.R. Greenwood, and J.P. McNeece, “Graphite Isotope Ratio Method Development Report: Irradiation Test Demonstration of Uranium as a Low Fluence Indicator”, PNNL-13488, Pacific Northwest National Lab (1999).
[4] C.J. Gesh, “A Graphite Isotope Ratio Method Primer-A Method for Estimating Plutonium Production in Graphite Moderated Reactors”, PNNL-14568, Pacific Northwest National Lab (2004).
[5] T.W. Wood, D.C. Gerlach, B.D Reid and, W.C Morgan, “Feasibility of Isotopic Measurements: Graphite Isotopic Ratio Method”, PNNL-13488, Pacific Northwest National Lab (2001).
[6] A. Aures, et al., Reactor simulations with nuclear data uncertainties, Nuclear Engineering and Design, Vol. 355, (2019)
[7] M. pusa, “Incorporating sensitivity and uncertainty analysis to a lattice physics code with application to CASMO-4”, Annals of Nuclear Energy, Vol 40, no.1, p. 153-162, (2012)
[8] M. L. Williams, et al., “A Statistical Sampling Method for Uncertainty Analysis with SCALE and XSUSA”, Nuclear Technology 183, p. 515–526, (2013)
[9] A.J. Koning, D. Rochman,” Towards sustainable nuclear energy: Putting nuclear physics to work”, Annals of Nuclear Energy Vol. 35, no. 11, p. 2024-2030, (2008)
[10] H. J. Shim, B. S. Han, J. S. Jung, H. J. Park, and C. H. Kim, “McCARD: Monte Carlo Code for Advanced Reactor Design Analysis”, Nuclear Engineering and Technology, Vol. 44, no. 2, p. 161-176, (2012)
[11] Somyung Park, Hyun Chul Lee, “Uncertainty Analysis for Graphite Isotope Ratio Method (GIRM) in the HANARO Simulation”, Korea Nuclear Society (KNS) Spring, (2024)
[12] H. J. Park, “McCARD/MIG stochastic sampling calculations for nuclear cross section sensitivity and uncertainty analysis”, Nuclear Engineering and Technology, Vol. 54 no. 11, p.4272-4279 (2022)
[13] Macfarlane, R., Muir, D. W., Boicourt, R. M., Kahler III, A. C., & Conlin, J. L. The NJOY nuclear data processing system, version 2016 (No. LA-UR-17-20093). Los Alamos National Lab. (LANL), Los Alamos, NM (United States), (2017).